Current Research in Food Science 8 (2024) 100653

Contents lists available at ScienceDirect

Current Research in Food Science

journal homepage: www.sciencedirect.com/journal/current-research-in-food-science

Enhancing pea protein isolate functionality: A comparative study of high-pressure homogenization, ultrasonic treatment, and combined processing techniques

Jun Yan [a], Sheliang Zhao [a], Xingfeng Xu [b,**], Fuguo Liu [a,*]

[a] College of Food Science and Engineering, Northwest A&F University, Yangling 712100, Shaanxi, PR China
[b] College of Food Science and Engineering, Qingdao Agricultural University, Qingdao, Shandong Province, 266109, PR China

ARTICLE INFO

Handling Editor: Dr. Maria Corradini

Keywords:
Pea protein
High-pressure homogenization
Ultrasonic treatment
Structure and function
Combined treatment

ABSTRACT

Pea protein has attracted widespread attention due to its high nutritional value, low allergenicity, non-GMO status, and broad availability. However, compared to animal proteins, pea protein has inferior functional properties, which limits its application in the food industry. This study used pea protein isolate (PPI) as the main raw material and investigated the effects of high-pressure homogenization (HPH), ultrasonic treatment (US), and the combination of the two in different orders on the structure and function of PPI. The results showed that HPH or US promoted the transformation of PPI insoluble suspension into a uniform protein dispersion, significantly reducing particle size, unfolding the spatial structure, exposing more amino acid residues. These structural changes resulted in a substantial increase in the solubility, foaming capacity and emulsifying activity of PPI. Moreover, the combined treatments further impacted the properties of PPI, largely depending on the order of the processing steps; the combination of HPH-US exhibited the best functional characteristics.

1. Introduction

In order to meet the nutritional demands of global population growth and ensure the sustainability of future food supply, plant protein has received extensive research attention (Sha and Xiong, 2020). Pea protein, in particular, has drawn significant interest due to its low allergenicity, high nutritional value, wide availability, and non-GMO status (Ge, et al., 2020; Lu et al., 2020). Despite being a high-quality nutritional source, the practicality of pea protein in food applications is still limited (Xiong, et al., 2018). Similar to most other plant proteins, poor solubility of commercial pea protein is a major obstacle to its widespread application in various food systems (Gao et al., 2022). Additionally, natural pea protein generally lacks high gelation (Ben-Harb et al., 2018) or emulsification capabilities (Karaca et al., 2011). This may be due to the compact structure of pea protein, which restricts its solubility and functionality, thus requiring structural improvement to overcome these limitations (Sha and Xiong, 2022).

High-pressure homogenization (HPH) and ultrasonic (US) treatment technologies have been widely used in food processing to alter the physicochemical and functional properties of proteins (Melchior et al., 2022; Xiong et al., 2018). HPH and US treatments can disrupt non-covalent interactions between proteins, reduce the size of protein aggregates, promote the formation of soluble supramolecular aggregates from insoluble protein aggregates, and at the same time, unfold the spatial structure of the protein to expose some reactive groups such as free sulfhydryl and hydrophobic groups, enhancing protein solubility, improving foaming and emulsifying properties (Shi et al., 2020; Chao et al., 2018).

Studies have shown that both HPH (Ong, et al., 2022) and US (Mozafarpour et al., 2022) have an impact on the physicochemical and functional properties of pea protein. The combined use of modification methods may be more effective in improving protein characteristics (Kamani et al., 2021). Zhao et al.'s study shows that the combination of HPH and US-assisted Maillard reaction can improve multiple functional properties of pea protein (Zhao, et al., 2022). In addition, recent research shows that the energy density level of nanoemulsions prepared by HPH-US combined technology is approximately half of the energy density level required by single HPH or US (Calligaris et al., 2018). Based on this, the combined HPH-US process has become a possible approach to reducing energy and cost while obtaining similar objective

* Corresponding author.
** Corresponding author.
E-mail addresses: jiaonanxuxingfeng@126.com (X. Xu), fuguo@nwafu.edu.cn (F. Liu).

https://doi.org/10.1016/j.crfs.2023.100653
Received 13 April 2023; Received in revised form 13 November 2023; Accepted 3 December 2023
Available online 7 December 2023

results. However, whether the combination of HPH and US treatment can further improve the functional properties of PPI, and the effect of processing sequence on PPI structure and function, remain unclear.

Therefore, this study aims to improve the structure and functional properties of commercial pea protein isolate (PPI) through HPH, US treatment, and their combination. The effects of different treatment methods on PPI structure were analyzed using methods such as particle size distribution, microstructure, surface hydrophobicity, intrinsic fluorescence spectroscopy, UV–visible absorption spectroscopy, and circular dichroism spectroscopy, and the solubility, foaming, and emulsifying properties of modified PPI were measured. The improvement in PPI functional properties was compared among single treatments, combined treatments, and different processing sequences. The method developed in this study aims to enhance the functional properties of plant protein, thus expanding its application in the food industry.

2. Materials and methods

2.1. Materials

Pea protein isolate (PPI, 90%) was purchased from Xi'an Zelong Biotech Co., Ltd. (Xian, China). Bovine serum albumin (BSA, 20 mg/mL) was purchased from Yuanye Biotechnology Co., Ltd. (Shanghai, China). Bicinchoninic acid (BCA) protein assay kit was obtained from Thermo Fisher Scientific (USA). 8-Aniline-1-naphthalene sulfonic acid (ANS) was obtained from Aladdin Biochemical Technology Co., Ltd. (Beijing, China). Corn oil was purchased from Luhua Group Co., Ltd. (Shandong, China).

2.2. High-pressure homogenization/ultrasonic treatment of PPI

PPI powder (1% w/v) was dispersed in deionized water and continuously stirred with a magnetic stirrer at 25 °C for 3 h. The pH of the sample solution was adjusted to 7.0 ± 0.2 using 1.0 M NaOH and left overnight at 4 °C. The samples suspension was treated using a high-pressure homogenizer (AH-BASIC II, SEEKER Industries, Canada) for three cycles at 50 MPa. Samples were promptly cooled in an ice-water bath after high-pressure homogenization. The samples suspension (30 mL) was also treated using an ultrasonic cell disruptor (JY92-IIDN, Huxie Industrial Co., LTD, Shanghai, China) at 20 kHz and 400 W ultrasonic power for 20 min, with the ultrasonic probe immersed about 2 cm below the samples suspension to avoid damage to the probe. The pulse cycle was set at 2 s of working time and 2 s of stopping time. Samples were placed in an ice-water bath to prevent overheating of the sample. The PPI treated with the high-pressure homogenizer was labeled as H-PPI. The PPI treated with ultrasonic treatment was labeled as U-PPI. Samples with combined HPH and US treatment were also prepared to investigate the effect of treatment sequence on PPI, with the sample treated with HPH first and US second labeled as HU-PPI and the sample treated with US first and HPH second labeled as UH-PPI.

2.3. Structural characteristics of modified PPI

2.3.1. Particle size distribution

The average particle size and particle size distribution of the samples were measured using a nano laser particle size analyzer (ZEN3600, Malvern Instruments, UK). The sample was diluted to 2 mg/mL and then placed in a particle size pool. The samples were equilibrated at 25 °C for 2 min before measurement, and the measurement was repeated three times.

2.3.2. Surface hydrophobicity

The surface hydrophobicity of samples was measured according to the method of Meng et al. (2021) with slight modifications. It was determined using 8-anilino-1-naphthalenesulfonic acid (ANS) as a fluorescence probe. The samples were diluted to 0.1, 0.2, 0.3, 0.4, and 0.5 mg/mL. A 4 mL sample solution was mixed with 20 μL of an 8 mmol/L ANS solution. The mixture was reacted in the dark at room temperature for 5 min, and the fluorescence intensity of the sample was measured using a fluorescence spectrophotometer (F-7000, Hitachi, Japan). The excitation and emission wavelengths were set at 390 and 470 nm, respectively, with a slit width of 5.0 nm and a scan rate of 1200 nm/min. The relationship between the sample concentration and fluorescence intensity was plotted, with the protein concentration on the x-axis and the fluorescence intensity on the y-axis. The slope of the resulting curve represents the surface hydrophobicity (H_0).

2.3.3. Fluorescence spectra

The intrinsic fluorescence spectra of the samples were measured using a fluorescence spectrophotometer (F-7000, Hitachi, Japan) after diluting the samples to 1.0 mg/mL in PBS (10 mmol/L, pH 7.0). The excitation wavelength was set at 280 nm, and the emission wavelength was set at 290–400 nm with a slit width of 5 nm.

2.3.4. UV–vis absorption spectra

The UV–visible absorption spectra of PPI were measured using a UV–vis spectrophotometer (UV-2550, Shimadzu, Japan) with a resolution of 0.1 nm and stray light of less than 0.0003%. The protein suspension (1.25 mg/mL) was centrifuged at 5000 × *g* for 20 min to remove large particles before absorbance scanning (200–500 nm). Before UV–vis absorption scanning, the supernatant was adjusted to a protein concentration of 0.5 mg/mL.

2.3.5. Circular dichroism (CD)

The circular dichroism spectra (Chirascan V100, Applied Photophysics, UK) of the sample solutions (prepared in section 2.2) were recorded using a CD spectrometer with a 0.1 cm quartz cell at 20 °C. The spectra were scanned from 190 to 260 nm at a speed of 50 nm/min with a bandwidth of 1 nm. PBS buffer was used as a blank. The secondary structure of proteins was analyzed using the DichroWeb online tool by comparing the CD spectra of the control PPI and modified PPI (Ma, et al., 2020).

2.3.6. Scanning electron microscopy (SEM)

The freeze-dried samples were stuck onto a cylindrical aluminum stub with double-sided carbon tape. A thin layer of gold was sputtered onto the sample surface. The morphology of the protein was observed using a field emission scanning electron microscope (Nano SEM-450, Fei, American) at an accelerating voltage of 5 kV.

2.4. Physicochemical and functional properties of modified PPI

2.4.1. Solubility

The PPI dispersion prepared in Section 2.2 (pH 7.0) was centrifuged at 10,000 × *g* for 20 min at room temperature. The protein content of the supernatant and original sample was determined by the BCA assay. A standard solution of bovine serum albumin (0–2.0 mg/mL) was prepared. Liquid A and liquid B in the BCA quantitative kit (Thermo Fisher Technology Co., LTD, USA) were mixed at a volume ratio of 50:1. 5 μL of the sample was taken and added into the enzyme label plate, and then 100 μL of BCA reagent was added. The mixture was incubated at 37 °C for 30 min with shaking, and the absorbance was measured at 560 nm using a multifunctional microplate reader (Model 680, Bio-Rad, USA). The solubility (%) was defined as 100 × protein content in the supernatant/total protein concentration.

2.4.2. Foaming properties

The foaming properties of the protein were determined according to the method of Shi et al. (2020). The prepared sample solution (V_0 mL) was homogenized at 10,000 r/min for 2 min using a high-speed homogenizer, and the foam volume obtained was recorded as V_1. After 30

min of static standing, the foam volume was recorded as V_2. The foaming ability (FA) and foam stability (FS) were calculated using the following equations:

$$FA\ (\%) = \frac{V_1 - V_0}{V_0} \times 100 \quad (1)$$

$$FS\ (\%) = \frac{V_2 - V_0}{V_1 - V_0} \times 100 \quad (2)$$

2.4.3. Emulsifying properties

The emulsifying properties of the protein were determined according to the method of Han et al. (2020) with slight modifications. The sample solution was diluted with distilled water to a concentration of 1 mg/mL, and 15 mL of the sample solution was mixed with 5 mL of corn oil. After homogenization at 10,000 r/min for 2 min using a high-speed shear homogenizer (Ultra Turrax T25, IKA, Staufen, Germany), 50 μL of the emulsion at the bottom of the container was mixed with 5 mL of SDS solution (0.1 wt%) and the absorbance was measured at 500 nm (UVmini-1240, Shimadzu, Japan). After 10 min of static standing, the emulsion (50 μL) at the bottom of the container was mixed with 5 mL of SDS solution (0.1 wt%), and the absorbance was measured at 500 nm. A 0.1 wt% SDS solution was used as a control. The emulsifying activity index (EAI) and emulsifying stability index (ESI) were calculated as follows:

$$EAI\ \left(m^2/g\right) = \frac{2 \times 2.303 \times A_0}{C \times (1 - \Phi) \times 10^4} \times dilution\ factor \quad (3)$$

$$ESI\ (\%) = \frac{A_{10}}{A_0} \times 100 \quad (4)$$

Where A_0 and A_{10} represent the absorbance at 0 and 10 min, respectively; C represents the protein concentration (g/mL); Φ represents the proportion of oil phase, which is 0.25 in this study.

2.5. Statistical analysis

The experimental results are expressed in terms of an average of three measurements. IBM SPSS 20 software (IBM, USA) was used for one-way analysis of variance (ANOVA), and Duncan's multiple comparison test was used to compare means. A p-value less than 0.05 was considered to indicate significant differences in the data. Origin 2019b software (OriginLab Corporation, USA) was used for plotting.

3. Results and discussion

3.1. Sample appearance and particle size distribution

Commercial pea protein isolate (PPI) has poor water solubility, with most proteins settling to the bottom of the glass vial after overnight storage at 4 °C. However, after PPI suspension was subjected to HPH or US treatment, a uniform PPI dispersion was obtained with no settling at the bottom of the vial (Fig. 1). This may be due to the significant reduction in particle size of PPI after HPH or US treatment (Fig. 2).

As shown in Fig. 2a, the average particle size of untreated PPI suspension was relatively large (>1000 nm), but was reduced to 1/4 of the original average size (approximately 200 nm) after HPH or US treatment, with a smaller PDI value. This may be due to the impact of shear and cavitation effects on PPI molecules during HPH or US treatment (Chen et al., 2016; Jiang et al., 2017). The turbulence and high-energy shear force produced by the cavitation effect could help to eliminate protein aggregation through the disruption of hydrogen bonds, hydrophobic interactions, and electrostatic interactions (Gao, et al., 2022; Wu et al., 2020), resulting in smaller average particle sizes and narrower size distributions. The smaller average particle size indicates the presence of particles with a larger surface area (Cheng et al., 2022). Additionally, there was no significant difference in average particle size and polydispersity index between the combined treatment and the single treatment conditions. The particle size distribution of untreated and treated PPI is shown in Fig. 2b. The intensity distribution data was measured, because it provides a more accurate measurement of particle size distribution when there are larger particles in the sample. The main peaks of the H, U, HU and UH groups are shifted to the left relative to the PPI samples, indicating the effectiveness of these treatments in reducing PPI average particle size.

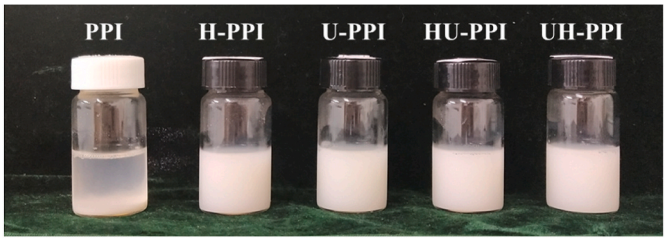

Fig. 1. Appearance of PPI suspensions after different physical treatments.

3.2. Structural characteristics of modified PPI

3.2.1. Microstructure

The SEM images of PPI and modified PPI in freeze-dried samples are shown in Fig. 3. After being freeze-dried, PPI suspension presented irregular particles of different sizes under the microscope, and these irregular large particles were difficult to disperse and settled to the bottom of the container after standing (Fig. 1). However, after being treated with HPH or US, the particle size significantly decreased, enabling them to disperse in aqueous solution to form a uniform PPI dispersion (Fig. 2). It is worth noting that the surface of PPI modified by HPH was rougher and more granular, while that modified by US was smoother. Under the joint processing conditions, PPI was connected by uniform small particles to form a smooth sheet-like structure, where the surface of HU-PPI was smoother, while that of UH-PPI was slightly granular, suggesting that the post-processing steps had a significant impact on the morphological structure of PPI.

3.2.2. Intrinsic fluorescence spectroscopy

Intrinsic fluorescence spectroscopy can determine changes in the tertiary spatial structure of protein molecules by detecting changes in intrinsic fluorescence intensity and maximum absorption wavelength in the spectrum (Shi, et al., 2020). Fluorescence intensity can display changes in the fluorescence quantum yield of aromatic amino acid residues (tryptophan, tyrosine, and phenylalanine) with different environmental hydrophobicity (Huang et al., 2015). The effects of HPH and US treatment on the intrinsic fluorescence spectra of PPI are shown in Fig. 4a. It can be observed that the position of the maximum absorption peak is not significantly different, indicating that HPH/US alone and HPH-US combined treatment have no effect on the maximum absorption wavelength of PPI intrinsic fluorescence, which is consistent with Shi et al.'s work (2020).

The intrinsic fluorescence intensity of PPI increased after HPH or US treatment (Fig. 4a), which may be due to the unfolding of the tertiary structure of PPI, and more chromophoric groups (such as tryptophan) were exposed to the solvent. The intrinsic fluorescence of PPI was further enhanced by combined treatment, indicating further unfolding of the tertiary structure of PPI. This is because the cavitation effect during HPH or US treatment destroys the protein structure, resulting in an increase in the number of chromophoric groups exposed to the solvent (Xiong, et al., 2018). This is consistent with the results of Shi et al., who reported an increase in intrinsic fluorescence intensity of whey protein isolate after HPH or US treatment, while the maximum absorption wavelength remained unchanged (Shi, et al., 2020). In addition, Cheng et al. (2022) reported that under HPH conditions, with the

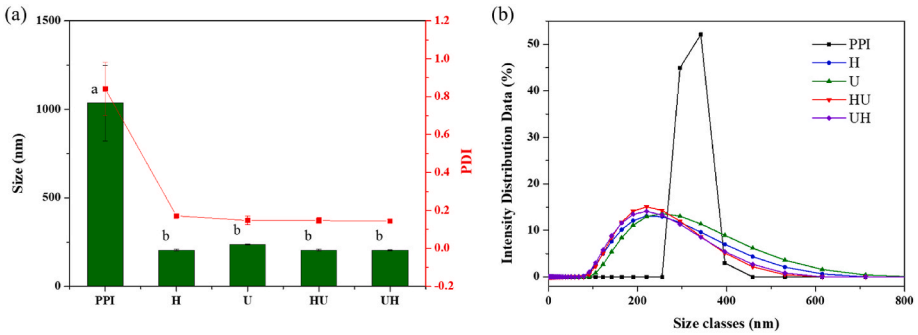

Fig. 2. (a) Average particle size and polydispersion index, (b) particle size distribution of PPI after different physical treatments.

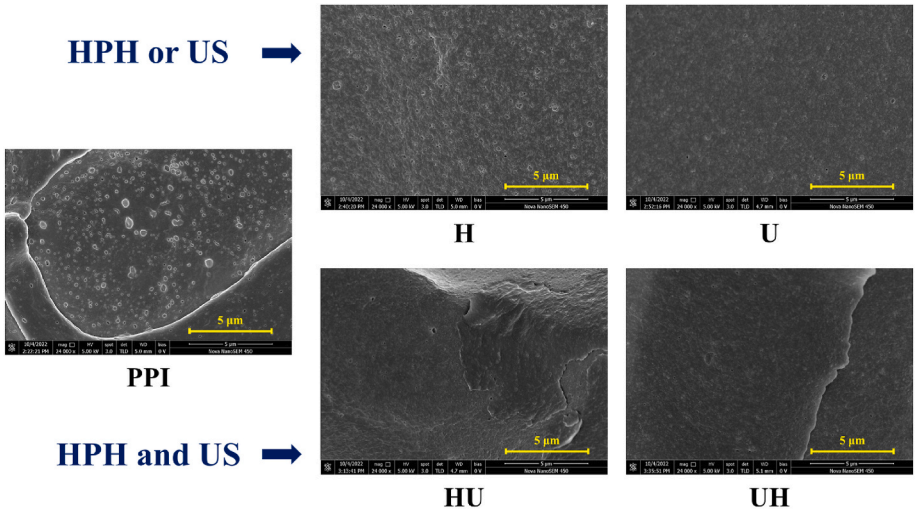

Fig. 3. Scanning electron micrographs of freeze-dried PPI samples which had been treated with high-pressure homogenization and ultrasound, singly and in combination.

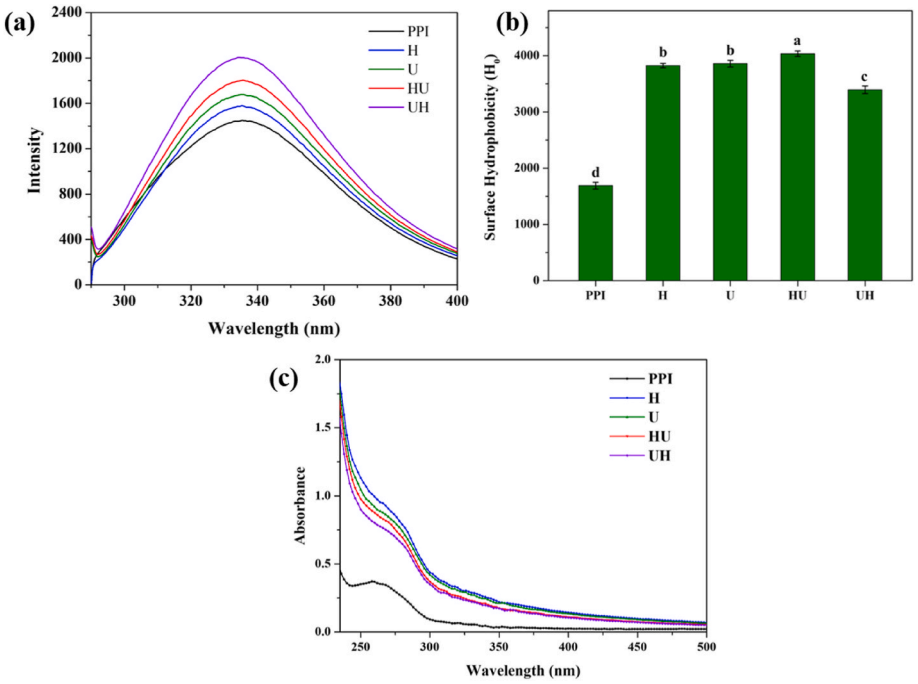

Fig. 4. (a)The intrinsic fluorescence spectra of PPI solution after different physical treatments; (b) Surface hydrophobicity of PPI after different physical treatments; (c) UV–vis absorption spectra of PPI after different physical treatments.

increase of processing pressure, the intrinsic fluorescence intensity of PPI increased significantly. However, it should be noted that the effect of HPH on protein intrinsic fluorescence intensity is controversial (Cheng et al., 2022). Han et al. (2020) showed that both HPH and US treatment reduced the fluorescence intensity of casein. These different results may be due to different processing environments (such as temperature control and homogenization process) and different amino acid composition of proteins. It is worth noting that the processing sequence also has a significant effect on the intrinsic fluorescence intensity of PPI, with the sample UH treated with US first having the highest intrinsic fluorescence intensity.

3.2.3. Surface hydrophobicity

The degree of surface hydrophobicity can reflect the number of hydrophobic groups exposed to polar solvents in a protein (Shi, et al., 2020). Changes in surface hydrophobicity of PPI after HPH and US treatment were detected using an exogenous fluorescence probe, ANS. When the probe binds to the accessible hydrophobic region of the protein, an increase in fluorescence intensity can be observed to determine the surface hydrophobicity of the protein (Alizadeh-Pasdar and Li-Chan, 2000). As shown in Fig. 4b, an increase in surface hydrophobicity in PPI following HPH, US, and combined treatments. The HU group exhibited the highest surface hydrophobicity, suggesting that HPH and US treatments could expose more hydrophobic amino acid residues. Both HPH and US treatment can significantly increase the surface hydrophobicity of PPI. An increase in the surface hydrophobicity indicates the exposure of the nonpolar amino acid side chain groups of amino acid residues (Jiang, et al., 2017). This may be due to that HPH and US treatment unfold the spatial structure of the protein, exposing more hydrophobic amino acid residues (mainly tryptophan residues) of PPI (Shi, et al., 2020). The exposed hydrophobic amino acid residues can improve the interaction between water and the protein (Han, et al., 2020), making it better dispersed in water, thereby achieving the goal of stabilizing the protein (Islam et al., 2019).

Interestingly, the surface hydrophobicity of the HU group, which underwent HPH first and then US treatment, further increased. In contrast, the surface hydrophobicity of the UH group, which underwent US treatment first and then HPH, was significantly reduced compared to the sample that underwent only single treatment. This also suggests that the two combined modification methods will further affect the spatial conformation of the protein (Dissanayake and Vasiljevic, 2009; Jiang et al., 2017), and US treatment seems to be more conducive to the exposure of hydrophobic amino acid residues in PPI. The weakening of the hydrophobicity of the UH sample may be related to the formation of hydrogen bonds between some hydrophilic amino acid residues on the surface of the protein molecule, boundary water molecules, and a decrease in hydrophobic regions (Han, et al., 2020). Although cavitation can also expose hydrophobic regions, it can gradually expose more hydrophilic groups embedded in the protein to the surface, leading to a decrease in surface hydrophobicity. Another reason may be that the exposed hydrophobic amino acid residues (such as tryptophan) form soluble protein aggregates due to hydrophobic interactions (Gao, et al., 2022).

3.2.4. UV–visible absorption spectroscopy

Proteins contain aromatic side chains of tyrosine, phenylalanine, and tryptophan, which can absorb ultraviolet light at 280 nm (Huang et al., 2019). Fig. 4c shows the UV–visible absorption spectra of PPI and physically modified PPI. Due to the combined effect of tyrosine (275 nm), tryptophan (279 nm), and phenylalanine (257 nm), a characteristic absorption peak is observed at 260–280 nm (Mozafarpour, et al., 2022). Any changes in the peak position or height after HPH or US treatment indicate changes in the microenvironment of aromatic amino acid residues (Han, et al., 2020).

Compared to PPI, physically modified PPI has a higher UV–visible absorption intensity. This may be due to HPH can cause changes in protein conformation due to the applied high pressure and shear forces, which in turn could expose more hydrophobic amino acid residues such as tryptophan, tyrosine, and phenylalanine on the surface of the protein molecule (Li et al., 2021; Zou et al., 2019). However, the UV absorbance of PPI treated with HPH and US (HU and UH) is lower than that of samples treated with only one method. This is because that long-term exposure to high-intensity US can oxidize sensitive functional groups, such as phenolic groups, which can reduce the UV absorbance of samples containing phenolic groups (Zhu, et al., 2018). Therefore, under strong cavitation effects, water produced by US wave breakdown may oxidize aromatic amino acids, especially tryptophan, tyrosine, and phenylalanine, thereby reducing absorbance (Mozafarpour, et al., 2022).

3.2.5. Circular dichroism spectroscopy

Circular dichroism (CD) spectroscopy is a widely used and convenient method that is sensitive to protein secondary structure and can be used to study conformational changes of proteins and peptides in solution (Provencher and Gloeckner, 1981). Like other plant globulins (Tang et al., 2009; Yue et al., 2021), PPI exhibits a relatively high content of β-sheet structure (Table 1). Compared to the control group, the β-sheet content of soluble aggregates induced by HPH and US treatment is significantly reduced, while the content of unordered coils is significantly increased, consistent with previous studies (Gao, et al., 2022; Melchior et al., 2022). In addition, PPI treated with only HPH shows the lowest content of β-sheets and the highest content of unordered coils, which may be due to the high sensitivity of pea protein secondary structure to pressure-induced hydrogen bond changes (Melchior, et al., 2022). Mechanical force can induce protein rearrangement and aggregation, resulting in different conformational structures stabilized by newly formed disulfide bonds and electrostatic interactions (Carullo, et al., 2020; Maresca et al., 2017; Panozzo et al., 2014). Intense shear and cavitation increase the kinetic energy and Brownian motion of proteins, increasing the collision frequency between protein molecules and promoting their aggregation, thereby reducing the content of β-sheet structure (Zhang, et al., 2022). In addition, in the collision of the HPH valve, turbulence, erosion, and high shear stress in the narrow gap can cause some damage to the folded structure, while US causes local high temperatures that force PPI to unfold, increasing its specific surface area and making it looser (Han, et al., 2020).

3.3. Physicochemical and functional properties of modified PPI

3.3.1. Solubility

Proteins are complex electrolytes with positive and negative charges that can be dispersed in water (Han, et al., 2020). Solubility is a specific manifestation of protein hydration, which is not only an effective indicator of protein conformational changes and aggregation properties, but also a favorable index for protein functionalities such as foaming, emulsifying, gelling, film-forming, and viscosity (Jambrak et al., 2008). It plays a crucial role in the development of new protein processing techniques and the creation of commercially valuable functional foods (Meng, et al., 2019). Commercial pea protein isolates differ greatly from natural proteins and are typically poorly soluble. Physical (shear

Table 1
Secondary structure contents of PPI after different physical treatments.

Sample	α-helix (%)	β-sheet (%)	β-turn (%)	random coil (%)
PPI	11.9 ± 0.36b	56.33 ± 0.12a	20.07 ± 0.21c	9.67 ± 0.06d
H	11.6 ± 0.17b	40.87 ± 1.3c	24.73 ± 0.4a	22.7 ± 1.3a
U	12.9 ± 0.1a	44.4 ± 0.1b	24.6 ± 0.1a	17.77 ± 0.06c
HU	13.23 ± 0.06a	44.37 ± 0.12b	24.97 ± 0.06a	16.97 ± 0.06c
UH	10.03 ± 0.83c	44.6 ± 0.26b	24.03 ± 0.25b	20.83 ± 1.19b

Different lowercase letters indicated significant differences in the content of the same secondary structure among different samples ($p < 0.05$).

mixing) and thermal stresses induced during protein extraction may alter the secondary/tertiary structure, leading to denaturation or partial denaturation of pea proteins (Tang, et al., 2009), which may result in the formation of very large polymeric protein particles in commercial PPIs (Gao, et al., 2022).

The solubility of modified PPIs obtained from HPH or US was three times higher that of commercial PPIs (Fig. 5a). This could be due to several factors: first, the cavitation, high shear, and turbulence induced by HPH or US treatment can induce larger aggregates to break down into smaller ones, making them more soluble (Luo et al., 2022a; Tang et al., 2009; Yang et al., 2018); second, mechanical and cavitation forces can disrupt hydrogen and hydrophobic bonds, causing partial cleavage or unfolding of the protein and exposing more surface area to interact with water molecules, thereby exposing more hydrophilic amino acid residues (Jambrak et al., 2009; Luo et al., 2022b; Tang et al., 2021); third, HPH or US treatment may increase the exposure of positively charged groups on the protein surface, resulting in stronger electrostatic repulsion between protein molecules and further enhancing protein solubility (Ong, et al., 2022).

It should be noted that whether HPH and US treatment can synergistically promote PPI solubility depends on the processing sequence. HU samples showed better solubility than single treatments, and this trend was consistent with the surface hydrophobicity (Fig. 4b). However, there was no significant difference between UH sample and single treatment sample. It has been well established that protein solubility depends on the extent of intermolecular interactions between hydrophobic regions on the protein surface, and when exposed hydrophobic groups participate in intermolecular interactions, solubility decreases. Conversely, when intermolecular interactions weaken, solubility increases, and surface hydrophobicity also increases (Hu, et al., 2013). HPH after US treatment may cause part of PPI to re-aggregate, forming a hydrophobic cross-linked protein network on the particle surface (Han, et al., 2020), thus reducing corresponding surface hydrophobicity and having no further effect on promoting dissolution.

3.3.2. *Foaming properties*

Proteins, as a powerful foaming agent, should have strong water solubility to stably adsorb at the air/water interface and form a thin film that protects the surrounding bubbles (Djemaoune et al., 2019). The evaluation of protein foaming properties includes two aspects: foaming ability (FA) and foam stability (FS). In theory, the transport, penetration, and recombination of protein molecules at the air/water interface are the main steps for protein foam formation. These processes are affected by protein particle size, surface hydrophobicity, and structural flexibility (Malik et al., 2017).

HPH and US treatment greatly increased the foaming ability of PPI, with the H and HU groups being the most optimal (Fig. 5b). The high-pressure homogenization and ultrasonic treatments are both able to induce protein unfolding, which exposes more hydrophobic groups to the protein surface. This could improve the foaming ability of PPI by enhancing protein-water interactions and protein adsorption at the air-water interface. Meanwhile, the reduction in particle size could facilitate the rapid migration of protein molecules to the air-water interface, thereby improving their foaming properties. (Saricaoglu et al., 2018; Han et al., 2020).

For the foam stability test at 30 min, HPH and HPH-US treatment significantly reduced the foam stability of the protein, possibly due to the long-time interval of the test. It has been reported in the literature that high-intensity US can induce partial unfolding of the protein structure, causing it to rapidly adsorb at the newly formed air/water interface and form a viscoelastic film, thereby obtaining greater foam stability within the first 10 min; as time goes on, the bubble size increases, and most of the PPI molecules desorb from the gas-liquid interface. Once they desorb from the interface, they are easily aggregated with other desorbed molecules through hydrophobic forces (Li, et al., 2017). Since more hydrophobic groups and hydrophobic regions are exposed to the surface during HPH or US treatment, the likelihood of protein aggregation is greatly increased. Foam-induced protein aggregation can reduce protein activity, resulting in similar foam stability to untreated PPI (Xiong, et al., 2018).

3.3.3. *Emulsifying properties*

Proteins can aid the mixing of two immiscible phases to form homogeneous emulsions in oil/water systems. The emulsification of proteins is evaluated based on two indices, emulsifying activity index (EAI) and emulsifying stability index (ESI). EAI is widely used to compare the emulsifying ability of proteins, where higher values indicate that proteins can rapidly adsorb at the oil droplet surface to form oil-water interfaces. ESI reflects the ability of proteins to prevent the separation of the resulting emulsion (Gao, et al., 2022). The change in emulsifying

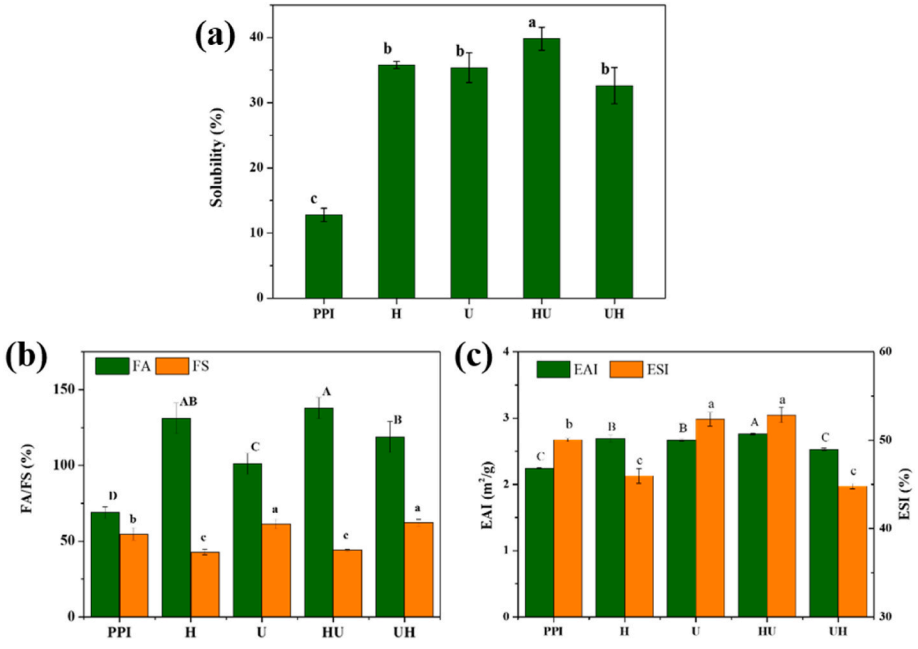

Fig. 5. The solubility (a), foaming (b), and emulsifying properties (c) of PPI after different physical modification.

properties is closely related to structural properties, solubility, surface hydrophobicity, oil-to-water ratio, and environmental pH (Chen et al., 2019).

Fig. 5c shows that HPH or US treatment enhances the emulsifying activity of PPI. The combined HPH-US treatment further increased the emulsifying activity of PPI, while the US-HPH treatment was less effective. EAI, as one of the important functional properties of proteins, usually depends on structural characteristics such as surface hydrophobicity and particle size (Jiang, et al., 2014). The smaller the protein particle size, the better its emulsification effect (Han, et al., 2020). An increase in surface hydrophobicity can enhance the hydrophobic interaction between adjacent protein molecules at the interface, thus improving the emulsifying activity (Shen et al., 2017). In this study, HPH or US treatment reduced the particle size of PPI (Fig. 2) and increased its surface hydrophobicity (Fig. 4b), making PPI more easily adsorbed at the oil-water interface (Luo, et al., 2022a; Shi et al., 2020). These treatments also increased the solubility of PPI, implying an increase in protein concentration in the dispersed phase of the O/W emulsion. Moreover, the US-HPH treatment was less effective than the individual treatments, which was consistent with the changes in surface hydrophobicity and solubility. This may be mainly attributed to the alteration of hydrophilic lipophilic balance (HLB) value induced by HPH after US treatment, reducing its ability to stabilize at the oil-water interface.

Compared with the original PPI, the emulsifying stability of high pressure homogenized PPI significantly decreased, while that of US-treated PPI significantly increased. The emulsifying stability of the combined treatment samples depends on the order of the post-treatment steps (HPH-US or US-HPH treatment). It is speculated that the protein re-aggregation induced by HPH may lead to a decrease in protein flexibility, which is an important factor affecting emulsifying stability (Wang, et al., 2008). Overall, the sample (HU-PPI) treated with HPH followed by US had the highest emulsifying activity index and the relatively strong emulsifying stability.

4. Conclusions

The present study aimed to improve the structure and functional properties of commercial PPI through HPH and US, and to analyze whether the combined treatment had a synergistic effect. The results showed that HPH or US could transform the PPI insoluble suspension into a uniform protein dispersion, presenting as uniform spherical particles under SEM. The treatments reduced the particle size of PPI through cavitation effects, high shear forces, and turbulence, which led to the expansion of the spatial structure of PPI and the exposure of more hydrophobic amino acid residues on the surface of PPI. In addition, the combined treatment had a further effect on the structural properties of the protein, which depended largely on the order of the post-treatment steps (HPH-US or US-HPH treatment). Furthermore, HPH or US greatly improved the solubility and foaming ability of commercial PPI. The synergistic treatment of HPH followed by US (HU-PPI) showed the best functional properties among all treatments. In summary, these findings have important implications for the food industry, particularly in the development of plant-based food products, such as meat substitutes, dairy alternatives, and protein-enriched baked goods. By enhancing the solubility, foaming, and emulsifying characteristics of PPI, there exists the potential to elevate the texture, stability, and overall quality of these plant-based products, thus rendering them more appealing to consumers.

CRediT authorship contribution statement

Jun Yan: Conceptualization, Methodology, Investigation, Formal analysis, Writing – original draft. **Sheliang Zhao:** Investigation, Methodology, Formal analysis. **Xingfeng Xu:** Supervision. **Fuguo Liu:** Conceptualization, Writing – review & editing, Methodology, Visualization, Supervision.

Declaration of competing interest

The authors declare that they have no known competing financial interests or personal relationships that could have appeared to influence the work reported in this paper.

Data availability

Data will be made available on request.

Acknowledgments

The authors gratefully acknowledge the financial support provided by the Major science and technology projects in the Xinjiang Uygur Autonomous Region (No. 2022A02004) and the Breeding Plan of Shandong Provincial Qingchuang Research Team (2021 Innovation Team of Functional Plant Protein-Based Food).

References

Alizadeh-Pasdar, N., Li-Chan, E.C., 2000. Comparison of protein surface hydrophobicity measured at various pH values using three different fluorescent probes. J. Agric. Food Chem. 48 (2), 328–334.

Ben-Harb, S., Panouille, M., Huc-Mathis, D., Moulin, G., Saint-Eve, A., Irlinger, F., Bonnarme, P., Michon, C., Souchon, I., 2018. The rheological and microstructural properties of pea, milk, mixed pea/milk gels and gelled emulsions designed by thermal, acid, and enzyme treatments. Food Hydrocolloids 77, 75–84.

Calligaris, S., Plazzotta, S., Valoppi, F., Anese, M., 2018. Combined high-power ultrasound and high-pressure homogenization nanoemulsification: the effect of energy density, oil content and emulsifier type and content. Food Res. Int. 107, 700–707.

Carullo, D., Donsì, F., Ferrari, G., 2020. Influence of high-pressure homogenization on structural properties and enzymatic hydrolysis of milk proteins. LWT 130, 109657.

Chao, D., Jung, S., Aluko, R.E., 2018. Physicochemical and functional properties of high pressure-treated isolated pea protein. Innovat. Food Sci. Emerg. Technol. 45, 179–185.

Chen, W., Wang, W., Ma, X., Lv, R., Watharkar, R.B., Ding, T., Ye, X., Liu, D., 2019. Effect of pH-shifting treatment on structural and functional properties of whey protein isolate and its interaction with (−)-epigallocatechin-3-gallate. Food Chem. 274, 234–241.

Chen, X., Xu, X., Zhou, G., 2016. Potential of high pressure homogenization to solubilize chicken breast myofibrillar proteins in water. Innovat. Food Sci. Emerg. Technol. 33, 170–179.

Cheng, J., Li, Z., Wang, J., Zhu, Z., Yi, J., Chen, B., Cui, L., 2022. Structural characteristics of pea protein isolate (PPI) modified by high-pressure homogenization and its relation to the packaging properties of PPI edible film. Food Chem. 388, 132974.

Dissanayake, M., Vasiljevic, T., 2009. Functional properties of whey proteins affected by heat treatment and hydrodynamic high-pressure shearing. J. Dairy Sci. 92 (4), 1387–1397.

Djemaoune, Y., Cases, E., Saurel, R., 2019. The effect of high-pressure microfluidization treatment on the foaming properties of pea albumin aggregates. J. Food Sci. Technol. 84 (8), 2242–2249.

Gao, K., Rao, J., Chen, B., 2022. Unraveling the Mechanism by Which High Intensity Ultrasound Improves the Solubility of Commercial Pea Protein Isolates. Food Hydrocolloids, 131, 107823.

Ge, J., Sun, C.X., Corke, H., Gul, K., Gan, R.Y., Fang, Y., 2020. The health benefits, functional properties, modifications, and applications of pea (Pisum sativum L.) protein: current status, challenges, and perspectives. Compr. Rev. Food Sci. Food Saf. 19 (4), 1835–1876.

Han, T., Wang, M., Wang, Y., Tang, L., 2020. Effects of high-pressure homogenization and ultrasonic treatment on the structure and characteristics of casein. LWT 130, 109560.

Hu, H., Wu, J., Li-Chan, E.C., Zhu, L., Zhang, F., Xu, X., Fan, G., Wang, L., Huang, X., Pan, S., 2013. Effects of ultrasound on structural and physical properties of soy protein isolate (SPI) dispersions. Food Hydrocolloids 30 (2), 647–655.

Huang, L., Ding, X., Li, Y., Ma, H., 2019. The aggregation, structures and emulsifying properties of soybean protein isolate induced by ultrasound and acid. Food Chem. 279, 114–119.

Huang, N., Cheng, X., Hu, W., Pan, S., 2015. Inactivation, aggregation, secondary and tertiary structural changes of germin-like protein in Satsuma mandarine with high polyphenol oxidase activity induced by ultrasonic processing. Biophys. Chem. 197, 18–24.

Islam, M.M., Kobayashi, K., Kidokoro, S.I., Kuroda, Y., 2019. Hydrophobic surface residues can stabilize a protein through improved water–protein interactions. FEBS J. 286 (20), 4122–4134.

Jambrak, A.R., Lelas, V., Mason, T.J., Krešić, G., Badanjak, M., 2009. Physical properties of ultrasound treated soy proteins. J. Food Eng. 93 (4), 386–393.
Jambrak, A.R., Mason, T.J., Lelas, V., Herceg, Z., Herceg, I.L., 2008. Effect of ultrasound treatment on solubility and foaming properties of whey protein suspensions. J. Food Eng. 86 (2), 281–287.
Jiang, L., Wang, J., Li, Y., Wang, Z., Liang, J., Wang, R., Chen, Y., Ma, W., Qi, B., Zhang, M., 2014. Effects of ultrasound on the structure and physical properties of black bean protein isolates. Food Res. Int. 62, 595–601.
Jiang, S., Ding, J., Andrade, J., Rababah, T.M., Almajwal, A., Abulmeaty, M.M., Feng, H., 2017. Modifying the physicochemical properties of pea protein by pH-shifting and ultrasound combined treatments. Ultrason. Sonochem. 38, 835–842.
Kamani, M.H., Semwal, J., Khaneghah, A.M., 2021. Functional modification of grain proteins by dual approaches: Current progress, challenges, and future perspectives. Colloid Surface B. 211, 112306.
Karaca, A.C., Low, N., Nickerson, M., 2011. Emulsifying properties of chickpea, faba bean, lentil and pea proteins produced by isoelectric precipitation and salt extraction. Food Res. Int. 44 (9), 2742–2750.
Li, R., Chang, Y., Zhang, L., Zhang, Y., Zhu, Y., Wang, T., 2017. Increase of bubble size playing a critical role in foam-induced protein aggregation: Aggregation of BSA in foam fractionation. Chem. Eng. Sci. 174, 387–395.
Li, W., Yang, H., Coldea, T.E., Zhao, H., 2021. Modification of structural and functional characteristics of brewer's spent grain protein by ultrasound assisted extraction. LWT 139, 110582.
Lu, Z., He, J., Zhang, Y., Bing, D., 2020. Composition, physicochemical properties of pea protein and its application in functional foods. Crit. Rev. Food Sci. Nutr. 60 (15), 2593–2605.
Luo, L., Cheng, L., Zhang, R., Yang, Z., 2022a. Impact of high-pressure homogenization on physico-chemical, structural, and rheological properties of quinoa protein isolates. Food Struct. 32, 100265.
Luo, L., Wang, Z., Deng, Y., Wei, Z., Zhang, Y., Tang, X., Liu, G., Zhou, P., Zhao, Z., Zhang, M., 2022b. High-pressure homogenization: a potential technique for transforming insoluble pea protein isolates into soluble aggregates. Food Chem. 397, 133684.
Ma, X., Hou, F., Zhao, H., Wang, D., Chen, W., Miao, S., Liu, D., 2020. Conjugation of soy protein isolate (SPI) with pectin by ultrasound treatment. Food Hydrocolloids 108, 106056.
Malik, M.A., Sharma, H.K., Saini, C.S., 2017. High intensity ultrasound treatment of protein isolate extracted from dephenolized sunflower meal: effect on physicochemical and functional properties. Ultrason. Sonochem. 39, 511–519.
Maresca, P., Ferrari, G., Júnior, B.R.d.C.L., Zanphorlin, L.M., Ribeiro, L.R., Murakami, M. T., Cristianini, M., 2017. Effect of dynamic high pressure on functional and structural properties of bovine serum albumin. Food Res. Int. 99, 748–754.
Melchior, S., Moretton, M., Calligaris, S., Manzocco, L., Nicoli, M.C., 2022. High pressure homogenization shapes the techno-functionalities and digestibility of pea proteins. Food Bioprod. Process. 131, 77–85.
Meng, X., Li, T., Song, T., Chen, C., Venkitasamy, C., Pan, Z., Zhang, H.J., 2019. Solubility, structural properties, and immunomodulatory activities of rice dreg protein modified with sodium alginate under microwave heating. Food Sci. Nutr. 7 (8), 2556–2564.
Meng, Y., Liang, Z., Zhang, C., Hao, S., Han, H., Du, P., Li, A., Shao, H., Li, C., Liu, L., 2021. Ultrasonic modification of whey protein isolate: implications for the structural and functional properties. LWT 152, 112272.
Mozafarpour, R., Koocheki, A., Nicolai, T., 2022. Modification of grass pea protein isolate (Lathyrus sativus L.) using high intensity ultrasound treatment: structure and functional properties. Food Res. Int. 158, 111520.
Ong, K.S., Chiang, J.H., Sim, S.Y.J., Liebl, D., Madathummal, M., Henry, C.J., 2022. Functionalising insoluble pea protein aggregates using high-pressure homogenisation: effects on physicochemical, microstructural and functional properties. Food Struct. 34, 100298.
Panozzo, A., Manzocco, L., Calligaris, S., Bartolomeoli, I., Maifreni, M., Lippe, G., Nicoli, M.C., 2014. Effect of high pressure homogenisation on microbial inactivation, protein structure and functionality of egg white. Food Res. Int. 62, 718–725.
Provencher, S.W., Gloeckner, J., 1981. Estimation of globular protein secondary structure from circular dichroism. Biochemistry 20 (1), 33–37.
Saricaoglu, F.T., Gul, O., Besir, A., Atalar, I., 2018. Effect of high pressure homogenization (HPH) on functional and rheological properties of hazelnut meal proteins obtained from hazelnut oil industry by-products. J. Food Eng. 233, 98–108.
Sha, L., Xiong, Y., 2022. Comparative structural and emulsifying properties of ultrasound-treated pea (Pisum sativum L.) protein isolate and the legumin and vicilin fractions. Food Res. Int. 156, 111179.
Sha, L., Xiong, Y.L., 2020. Plant protein-based alternatives of reconstructed meat: Science, technology, and challenges. Trends Food Sci. Technol. 102, 51–61.
Shen, X., Shao, S., Guo, M., 2017. Ultrasound-induced changes in physical and functional properties of whey proteins. Int. J. Food Sci. Technol. 52 (2), 381–388.
Shi, R., Liu, Y., Hu, J., Gao, H., Qayum, A., Bilawal, A., Munkh-Amgalan, G., Jiang, Z., Hou, J., 2020. Combination of high-pressure homogenization and ultrasound improves physiochemical, interfacial and gelation properties of whey protein isolate. Innovat. Food Sci. Emerg. Technol. 65, 102450.
Tang, C., Wang, X., Yang, X., Li, L., 2009. Formation of soluble aggregates from insoluble commercial soy protein isolate by means of ultrasonic treatment and their gelling properties. J. Food Eng. 92 (4), 432–437.
Tang, S., Du, Q., Fu, Z., 2021. Ultrasonic treatment on physicochemical properties of water-soluble protein from Moringa oleifera seed. Ultrason. Sonochem. 71, 105357.
Wang, X., Tang, C., Li, B., Yang, X., Li, L., Ma, C., 2008. Effects of high-pressure treatment on some physicochemical and functional properties of soy protein isolates. Food Hydrocolloids 22 (4), 560–567.
Wu, D., Tu, M., Wang, Z., Wu, C., Yu, C., Battino, M., El-Seedi, H.R., Du, M., 2020. Biological and conventional food processing modifications on food proteins: structure, functionality, and bioactivity. Biotechnol. Adv. 40, 107491.
Xiong, T., Xiong, W., Ge, M., Xia, J., Li, B., Chen, Y., 2018. Effect of high intensity ultrasound on structure and foaming properties of pea protein isolate. Food Res. Int. 109, 260–267.
Yang, J., Liu, G., Zeng, H., Chen, L., 2018. Effects of high pressure homogenization on faba bean protein aggregation in relation to solubility and interfacial properties. Food Hydrocolloids 83, 275–286.
Yue, J., Gu, Z., Zhu, Z., Yi, J., Ohm, J.-B., Chen, B., Rao, J., 2021. Impact of defatting treatment and oat varieties on structural, functional properties, and aromatic profile of oat protein. Food Hydrocolloids 112, 106368.
Zhang, A., Wang, L., Song, T., Yu, H., Wang, X., Zhao, X.-h., 2022. Effects of high pressure homogenization on the structural and emulsifying properties of a vegetable protein: Cyperus esculentus L. LWT 153, 112542.
Zhao, S., Huang, Y., McClements, D.J., Liu, X., Wang, P., Liu, F., 2022. Improving pea protein functionality by combining high-pressure homogenization with an ultrasound-assisted Maillard reaction. Food Hydrocolloids 126, 107441.
Zhu, Z., Zhu, W., Yi, J., Liu, N., Cao, Y., Lu, J., Decker, E.A., McClements, D.J., 2018. Effects of sonication on the physicochemical and functional properties of walnut protein isolate. Food Res. Int. 106, 853–861.
Zou, J., Nguyen, N., Biers, M., Sun, G., 2019. Conformational changes of soy proteins under high-intensity ultrasound and high-speed shearing treatments. ACS Sustain. Chem. Eng. 7 (9), 8117–8125.